Transversal structure of a sum-frequency beam generated from the surface of a chiral medium

2009 J. Opt. A: Pure Appl. Opt. 11 074008

(http://iopscience.iop.org/1464-4258/11/7/074008)

J. Opt. A: Pure Appl. Opt. **11** (2009) 074008 (11pp) doi:10.1088/1464-4258/11/7/074008

Transversal structure of a sum-frequency beam generated from the surface of a chiral medium

V A Makarov[1,2] **and I A Perezhogin**[1]

[1] International Laser Center, M V Lomonosov Moscow State University, Leninskie Gory, Moscow 119991, Russia
[2] Faculty of Physics, M V Lomonosov Moscow State University, Leninskie Gory, Moscow 119991, Russia

E-mail: iap1@mail.ru

Received 20 October 2008, accepted for publication 29 January 2009
Published 6 May 2009
Online at stacks.iop.org/JOptA/11/074008

Abstract

In this work we study sum-frequency generation from the surface of an isotropic chiral medium in arbitrary interaction geometry of the paraxial light beams at fundamental frequencies. The analytical formulae have been deduced completely describing the transversal spatial distribution of the electric field in the light beam at sum-frequency. Even in a zero-order approximation on the divergence angles of the beams the transversal spatial intensity distribution in the signal beam is elliptic Gaussian, and its shape depends only on the geometry of incidence, the transversal dimensions and the frequencies of the fundamental beams.

Within the first-order approximation approach, generally, the polarization state of light is distributed inhomogeneously in the reflected signal beam cross section, and the transversal intensity distribution is not Gaussian. But when the fundamental beams are not focused tightly enough, the non-Gaussian part of the field is negligibly small, compared to the Gaussian part with uniform polarization distribution. However, at larger angles of incidence the non-Gaussian contribution becomes comparable with the Gaussian zero-order part of the field (or exceeds it) even in the case of slightly focused fundamental beams. In this case the transversal distributions of intensity and polarization of light become very sophisticated.

Keywords: polarization, chirality, sum-frequency, surface, light beam, transversal effects

(Some figures in this article are in colour only in the electronic version)

1. Introduction

Sum-frequency generation (SFG) is the efficient and well-known method of surface diagnostics. It is widely used in the spectroscopy of surfaces and interfaces (see, for example, [1–3]), in microscopy [4–6], for surface plasmon excitation [7], for the examination of the orientation of molecules and of other objects [8, 9] at the surfaces or interfaces. In connection with the above-mentioned problems, some of the research has also developed theoretical models of light interaction with the investigated molecules (see, for example, [8, 10]). The advantages of SFG as a tool for surface diagnostics are the possibility of application in an atmosphere (and also at high pressures), and good spatial precision (depending on the effective sizes of the fundamental beam waists).

The authors of different works have made attempts to take into account the spatial dispersion of the nonlinear optical response of a chiral medium [11–14], the inhomogeneity of the optical properties of the medium surface layer [15] and to find a method of experimental separation of the sum-frequency (SF) signal from the bulk of the medium and from its surface [16]. In [17] these problems have been overcome by the modified boundary conditions for the electromagnetic field at the surface of the medium. The substantiation and the details of such an approach are described in [18, 19].

The above-mentioned achievements in SFG research have been made mainly within the framework of the plane wave

approximation. At the same time, the result of SFG depends strongly on the effective size of the beam waists. From this point of view, the account for a spatial finiteness of incident and reflected beams seems to play a certain role. The importance of this issue is confirmed by the investigations of linear reflection and refraction of finite light beams. The first-order effects on the beam divergence angle lead to small deflections of the light beams from the trajectories predicted by geometrical optics in the reflection and refraction of these beams (see experimental work in [20]; also work in [21] for 2D beams and work in [22] for 3D beams; earlier work can be found in [1–7] of [21]). Moreover, the spatial finiteness of light beams leads to the appearance of a small inhomogeneity of the polarization distribution in the cross sections of reflected and refracted beams even in linear optical processes. Intense research in this area is also continuing at the present time [23–25]. Thus, the account of a spatial finiteness of the light beams in SFG reveals new interesting effects (especially concerning polarization) in the cross section of the reflected signal beam, which may appear to be vital in some cases for the correct interpretation of SFG experiments.

For the first time, the authors of [26] have taken into account the spatial finiteness of the light beams in a three-wave mixing process. They considered the second-harmonic generation (SHG) from the surface of a chiral medium with spatial dispersion of the nonlinearity in the case of the oblique incidence of a 2D light beam ('slit' beam) at fundamental frequency. Later, in [27] they investigated the SHG by normal incidence of a 3D fundamental beam. In both [26] and [27] the authors utilized the approach, presented in [18, 19], in order to describe the light–matter interaction. Afterwards, in [28] Makarov and Perezhogin have deduced and thoroughly analyzed the formulae completely describing the transversal distributions of the intensity and polarization in the second-harmonic beam. It was shown that the quantitative information about the relation of the nonlinear optical susceptibilities of the medium can be extracted directly from the polarization distribution in the cross section of the signal beam at double frequency. One should note that the other methods (as a measurement of the intensity of the SF signal (or its circularly polarized components), or measurement of the mean polarization of the SF beam) delivering the same information, usually result in the necessity of solving cumbersome algebraic equations.

Thus, basing on the results of the studies of the oblique incidence of a 2D beam [26] and the normal incidence of a 3D beam [27, 28] it can be concluded, that in the case of the normal incidence of both of the pump beams the SFG is forbidden within the plane wave approximation. Under this condition the signal beam appears only owing to the spatial finiteness (and focusing) of pump beams, as a result of the interaction of non-collinear spatial Fourier components of the light field. In this case, the signal beam is non-Gaussian and it is inhomogeneously polarized, so that the polarization state of light significantly changes at relatively small distances within the area of the beam cross section. As for the oblique incidence (which is the most widespread case of SFG) of real 3D fundamental beams, it can only be supposed (considering the results of [26] for 2D beams) that, probably, the plane wave approximation provides a good quantitative description of the power of the signal beam and its polarization, because the non-Gaussian part of the field is expected to be negligible compared with the Gaussian one.

One of the main goals of our work is to answer the question finally, when such an assumption is true, and what are the borders of the applicability of the plane wave approximation in this task? In order to completely solve this problem we need to obtain an analytical formula, fully describing the transversal distribution of the electric field in the reflected beam at SF in the case of SFG by oblique incident elliptically polarized beams. In certain cases the results of this study may prevent researchers from a wrong interpretation of experimental data, obtained as a mean value of the polarization of radiation at SF. Moreover, as was found in earlier studies of SHG and SFG in chiral media [28, 29], the attractiveness of the solution of the discussed problem is provided by the appearance of the new polarization effects in the signal beam cross section, which potentially can give more information about the investigated chiral medium.

2. General description of the solution of the problem

The reflected signal beam at the SF appears due to the nonlinear optical response of the surface and due to the nonlinear (local and nonlocal) optical response of the medium bulk (that is, due to the nonlinear polarization of the medium provided by the refracted fundamental waves). Various approaches can be used in order to correctly describe all the contributions from the surface and from the bulk. We use the method, described in [18], which utilizes the so-called modified boundary conditions for the electromagnetic field. The latter are obtained by the solution of the Maxwell equations for the monochromatic wave at frequency $\omega = 2\pi\, c/\lambda$ (c is velocity of light in vacuum and λ is the wavelength of light) in the inhomogeneous surface layer of the nonlinear medium. These equations are solved within the first-order approximation on d_0/λ, where $d_0 \ll \lambda$ is the effective thickness of this layer:

$$\begin{aligned} \mathbf{E}_{\mathrm{tan}}(2) - \mathbf{E}_{\mathrm{tan}}(1) &= \frac{4\pi}{\mathrm{i}\omega}\mathrm{grad}_{\mathrm{tan}}(i_n), \\ D_n(2) - D_n(1) &= \frac{4\pi}{\mathrm{i}\omega}\mathrm{div}(\mathbf{i}_{\mathrm{tan}}), \\ \mathbf{B}(2) - \mathbf{B}(1) &= -\frac{4\pi}{c}[\mathbf{n}\times\mathbf{i}_{\mathrm{tan}}], \end{aligned} \tag{1}$$

where $\mathbf{E}(2)$, $\mathbf{D}(2)$ and $\mathbf{B}(2)$ are the values of the electric field, the electric displacement and the magnetic field at the surface inside medium 2, and $\mathbf{E}(1)$, $\mathbf{D}(1)$ and $\mathbf{B}(1)$ are the values of the same quantities at the surface inside medium 1. Indexes tan and n designate tangential and normal components of vectors in (1); $\mathbf{n}$ is the unit vector, perpendicular to the surface, directed from medium 1 to medium 2; $\mathbf{i}$ can be interpreted as a surface current density of the bounded charges. $\mathbf{i}$ is proportional to the first order of d_0/λ. In our case, when medium 1 is a vacuum, we can represent $\mathbf{i}$ as the following series:

$$\mathbf{i} = \kappa^{(1)}\cdot\mathbf{E}^{\mathrm{v}} + \kappa^{(2)}:\mathbf{E}^{\mathrm{v}}\mathbf{E}^{\mathrm{v}} + \kappa^{(3)}\vdots\mathbf{E}^{\mathrm{v}}\mathbf{E}^{\mathrm{v}}\mathbf{E}^{\mathrm{v}} + \cdots \tag{2}$$

where $\mathbf{E}^{\mathrm{v}}$ is the electric field at the surface in vacuum, and tensors $\hat{\kappa}^{(n)}$ characterize the surface response on the external electromagnetic field. $\hat{\kappa}^{(n)}$ are the material tensors: they do not depend on the angles of incidence and on the other parameters of the electromagnetic waves.

Because we consider the quadratic nonlinear optical response, the expressions for the nonlinear surface current density and for the nonlinear polarization will be given as follows:

$$\begin{aligned} i_j^{\mathrm{NL}} &= \kappa^{(2)}_{jkl}\mathbf{E}^{\mathrm{v}}_{1k}\mathbf{E}^{\mathrm{v}}_{2l} \\ P_i^{\mathrm{NL}} &= \chi^{(2)}_{ijk}\mathbf{E}^{t}_{1j}\mathbf{E}^{t}_{2k} + \gamma^{(2)1}_{ijkl}\frac{\partial \mathbf{E}^{t}_{1k}}{\partial x_j}\mathbf{E}^{t}_{2l} + \gamma^{(2)2}_{ijkl}\mathbf{E}^{t}_{1k}\frac{\partial \mathbf{E}^{t}_{2l}}{\partial x_j}, \end{aligned} \tag{3}$$

where $\mathbf{E}^{t}_{1,2}$ are the electric fields at the fundamental frequencies $\omega_{1,2}$ inside the medium (the fields of the refracted waves) at the surface, and $\mathbf{E}^{\mathrm{v}}_{1,2}$ are the electric fields in vacuum at the surface (they are the superpositions of the reflected and of the incident waves); $\chi^{(2)}_{ijk}$ is the tensor of the local quadratic optical susceptibility of the medium bulk; $\gamma^{(2)1}_{ijkl} = \gamma^{(2)}_{ijkl}(\omega_1+\omega_2;\omega_1,\omega_2)$ and $\gamma^{(2)2}_{ijkl} = \gamma^{(2)}_{ijlk}(\omega_1+\omega_2;\omega_2,\omega_1)$; here $\gamma^{(2)}_{ijkl}(\omega_1+\omega_2;\omega_1,\omega_2)$ is the tensor of spatial dispersion of the quadratic optical response of the medium bulk (it describes the nonlocality of the nonlinear optical response; the details of the approach describing the spatial dispersion in terms of such a tensor can be found in [17, 19, 26–28]). In general, $\gamma^{(2)1}_{ijkl} \neq \gamma^{(2)2}_{ijkl}$. We note that $\gamma^{(2)}_{ijkl}(\omega_1+\omega_2;\omega_1,\omega_2)$ does not possess any permutation symmetry, connected with the corresponding permutation of the frequency arguments in it (unlike in $\chi^{(2)}_{ijk}(\omega_1+\omega_2;\omega_1,\omega_2) = \chi^{(2)}_{ikj}(\omega_1+\omega_2;\omega_2,\omega_1)$). The structure of the tensors $\kappa^{(2)}_{jkl}$, $\chi^{(2)}_{ijk}$ and $\gamma^{(2)}_{ijkl}$ is determined by the symmetry properties of the isotropic chiral medium; the non-zero components of these tensors for such a medium are given in the appendix of this paper.

In order to obtain the expressions for the electromagnetic field of the reflected wave at SF within the plane wave approximation, and within the approximation of non-depleting pump, we have to carry out the following steps. (a) We solve the equations for the electromagnetic field at the surface of the medium obtained from the conventional boundary conditions (which coincide with the modified ones, when the nonlinear polarization is zero and when we neglect the members of the order of d_0/λ and higher). Thus, we find the electric fields $\mathbf{E}^{t}_{1,2}$ at the surface inside the medium (refracted field) and $\mathbf{E}^{\mathrm{v}}_{1,2}$ at the surface in vacuum (superposition of the incident and reflected field). (b) We substitute these electric fields in equations (3) and obtain the nonlinear polarization of the medium bulk and the nonlinear response of the medium surface. Now we are able to substitute the nonlinear polarization and the nonlinear current density in the modified boundary conditions (1), which contain the reflected electric field at SF in the left part of the equations (in designations of (1) it appears as $\mathbf{E}_3(1)$). But there is also another unknown value, namely the electric field at SF inside the medium $\mathbf{E}_3(2)$. In order to find it, (c) we solve the wave equation with the nonlinear polarization of the medium bulk in the right part for the plane wave $\mathbf{E}_3(2)$, propagating in the medium bulk. Finally (d) we substitute the quantities found above (nonlinear polarization, nonlinear current density, $\mathbf{E}_3(2)$) to the modified boundary conditions (1). In the case of consideration of plane waves, (1) can be represented as algebraic equations for $\mathbf{E}_3(1)$. Thus, we find the reflected plane wave at SF from these equations at the surface of the medium. More details on steps (a)–(d) are given in [17], where this method has been used.

Suppose now we are considering finite light beams instead of plane waves, where the electromagnetic fields depend on the coordinates in space. Now we are able to carry out the same steps (a)–(d) when representing all the beams in this task as the superpositions of their spatial Fourier harmonics. In this case, when performing the steps (a)–(d), we will treat the spatial Fourier harmonics of the incident, the reflected and the refracted waves. Moreover, we assume that the angles of divergence of the light beams at fundamental frequencies are small and, therefore, the spatial Fourier harmonics propagating at sufficiently large angle (comparable to 1 rad) relative to the axis of any of the beams will have negligibly small amplitudes. In this case, since the incident beams can be represented in their reference frames as $\mathbf{E}_{1,2}(\mathbf{r}_{1,2}, z_{1,2}=0) = \int\int \tilde{\mathbf{E}}_{1,2}(\mathbf{k}_{1,2\perp})\exp\{\mathrm{i}\mathbf{k}_{1,2\perp}\mathbf{r}_{1,2}\}\,\mathrm{d}\mathbf{k}_{1,2\perp}$, we consider only small values of the transversal components $\mathbf{k}_{1,2\perp}$ of the wavevectors of the spatial Fourier harmonics, and we linearize all the algebraic equations appearing in (a)–(d) with respect to these components.

It is worth noticing that the nonlinear polarization and the nonlinear current density in (3) containing the products of the electric fields look like convolution products of these fields in a Fourier representation with the variables of integration $\mathbf{k}_{1,2\perp}$. Thus, (3) will represent the summation of all contributions of all interacting pairs of the Fourier harmonics of the fundamental waves, such that $\mathbf{k}_{1\perp} + \mathbf{k}_{2\perp} = \mathbf{k}_{3\perp}$. The latter condition imposes a constraint on the variables of integration.

3. The solution of the problem for uniformly polarized incident beams with Gaussian intensity profiles

Let us consider two monochromatic elliptically polarized Gaussian beams with small divergence angles such that the effective sizes of their widths are much bigger than the wavelength of light, $w_{1,2} \gg \lambda_{1,2}$. These beams at frequencies $\omega_{1,2}$ are falling onto the surface of the isotropic chiral medium, as is illustrated in figure 1. We designate the angles of incidence of these beams (i.e. the angles between the symmetry axes of these beams and the perpendicular to the surface) as $\theta_{1,2}$. The angle between the planes of incidence of these beams is designated as α_2. Let us choose the plane of incidence of the first beam coinciding with the coordinate plane $x^{\Pi}z^{\Pi}$ of the reference frame $x^{\Pi}y^{\Pi}z^{\Pi}$, bounded with the surface (z^{Π}-axis of this coordinate system is directed into the medium (see figure 1) and it is perpendicular to the surface). Also each beam will be associated with its 'own' reference frame ($x_1y_1z_1$ and $x_2y_2z_2$ correspondingly) as is shown for the first beam at figure 1.

The positions of the centers of the waists of the incident beams are chosen at $\{x_{1,2}=0;\ y_{1,2}=0;\ z_{1,2}=0;\}$

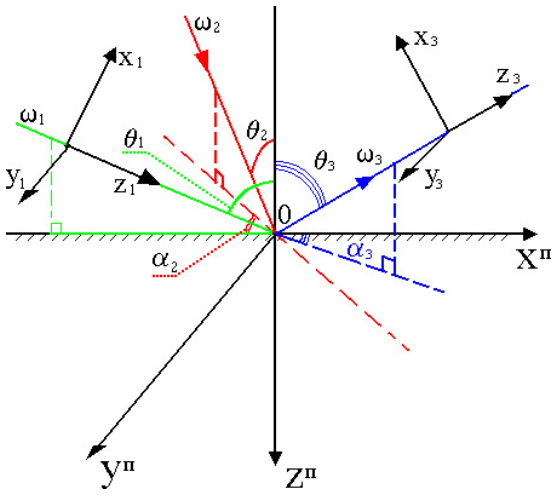

Figure 1. Scheme of the interaction of incident beams of radiation at fundamental frequencies and the orientation of the reference frames, attached to the incident and reflected beams, and to the surface.

correspondingly. Let these two points coincide with the zero of the surface reference frame $\{x^{\Pi} = 0;\ y^{\Pi} = 0;\ z^{\Pi} = 0;\}$. (Such an assumption is made only for clarifying the resulting expressions. The shifts of the spot centers of incident beams along the surface or along the axes of the beams can be easily accounted for. It can be shown that they lead to the weakening of the SF signal, to the shift of the center of the reflected SF beam, and to additional distortions of the transversal distribution of the light field at SF.)

In this case spatial distributions of the electric fields in their 'own' reference frames are given by the following expressions:

$$\mathbf{E}_m(x_m, y_m, z_m) = \left[\mathbf{e}_m + \frac{\mathrm{i}}{k^i_{1,2}}\mathbf{e}_z^{(m)}(\mathbf{e}_m \cdot \nabla)\right] \times \frac{E_{0m}}{\beta_m(z_m)} \exp\left\{\frac{-x_m^2 - y_m^2}{w_m^2\beta_m(z_m)} - \mathrm{i}\omega_m t + \mathrm{i}k^i_m z_m\right\} \quad (4)$$

where $m = 1,\ 2$ indicates the first or second incident beam, $\mathbf{e}_z^{(m)}$ is the unit vector along the positive direction of the z_m axis of the corresponding reference frame, $\mathbf{e}_m$ are the complex unit vectors ($|\mathbf{e}_m|^2 = 1$, $\mathbf{e}_m \perp \mathbf{e}_z^{(m)}$), defining the polarization state of light in the incident beams, E_{0m} are the amplitudes of the electric field of the incident beams, ω_m are the fundamental frequencies, w_m are the effective waists of the fundamental beams, $k_m = \omega_m/c$, $\beta_m(z_m) = 1 + 2\mathrm{i}z_m/(k^i_m w_m^2)$. The expression (4) also takes into account the longitudinal components of the fields at fundamental frequencies $\mathbf{E}_{1,2}$. Within the first-order approximation on the divergence angles of the beams, the Maxwell equations $\mathrm{div}\,\mathbf{E}_{1,2} = 0$ in vacuum for beams with Gaussian profiles can be satisfied only by taking into account the longitudinal component of the electric field (which is the first-order value).

In order to describe the polarization and the intensity of the incident pump beams (as well as for any other beams) it is convenient to use the following quantities: normalized intensity of light $I_{0m} = (|E_{m+}|^2 + |E_{m-}|^2)/2$, the ellipticity degree of the polarization ellipse of light $M_{0m} = (|E_{m+}|^2 - |E_{m-}|^2)/(|E_{m+}|^2 + |E_{m-}|^2)$, the angle of orientation of the main axis of the polarization ellipse $\Psi_m = \frac{1}{2}\mathrm{Arg}\{E_{m+}E^*_{m-}\}$ and the angle of orientation of the electric field vector at fixed timing $\Phi_m = \mathrm{Arg}\{E_{m+} + E^*_{m-}\}$. In these definitions $E_{m\pm} = E_{mx} \pm \mathrm{i}E_{my}$ are the circularly polarized amplitudes of the electric field. It is not difficult to show that the polarization vector of the fundamental beams can be written as $\mathbf{e}_m = \sqrt{\frac{1-M_{0m}}{2}}\,\mathrm{e}^{-\mathrm{i}\Psi_m}\mathbf{e}_+ + \sqrt{\frac{1+M_{0m}}{2}}\,\mathrm{e}^{\mathrm{i}\Psi_m}\mathbf{e}_-$, where M_{0m} are the initial values of the degree of ellipticity of their polarization ellipses, Ψ_{0m} are the initial values of orientation angles of their polarization ellipses and $\Phi_m = 0$ corresponds to the uniform phase distributions. M_{0m} change from -1 (circular polarization with counterclockwise rotation) to 1 (circular polarization with clockwise rotation) through 0 (linear polarization), and Ψ_{0m} vary from 0 to π (0 and π are indistinguishable).

Before we start with steps (a)–(d) described above, we obtain the Fourier representation of the transversal and the longitudinal constituents of the electric fields of the incident beams in their 'own' reference frames. Then we proceed to the reference frame bounded to the surface and transform all the quantities (the electric field and the wavevectors) in a corresponding way (of course, at this stage we take into account the dependence of spatial Fourier harmonics on the coordinates z_1 and z_2 in $x_1y_1z_1$ and $x_2y_2z_2$). At that, for any Fourier harmonic of each of the two beams its wavevector is given as $\mathbf{k}^i_m = \mathbf{k}_{m\perp} + k_{mz}\mathbf{e}_z^{(m)}$ in $x_my_mz_m$. In $x^{\Pi}y^{\Pi}z^{\Pi}$ the component of this wavevector, parallel to the surface $x^{\Pi}y^{\Pi}$, can be represented as the sum of a fixed value ($k^i_1 \sin\theta_1\mathbf{e}_x$ and $k^i_2 \sin\theta_2(\mathbf{e}_x\cos\alpha_2 + \mathbf{e}_y\sin\alpha_2)$ correspondingly) and of some small additive ($\tilde{\mathbf{k}}_{1\perp}$ and $\tilde{\mathbf{k}}_{2\perp}$ correspondingly), appearing due to the non-collinearity of the Fourier harmonics of each of the incident beams. We linearize all the equations respectively to this small additive $\tilde{\mathbf{k}}_{1\perp}$ and $\tilde{\mathbf{k}}_{2\perp}$ (except for the real part of the exponential index of the fields, where the first-order terms are zero for Gaussian beams).

Then we proceed to stages (a)–(d), and after completing them we switch to the reference frame of the reflected signal beam (see figure 1) with corresponding transformation of the electric field vector, wavevectors and coordinates. As far as we suppose small divergence angles of the incident beams, the propagation direction of the reflected SF beam (and the orientation of the reference frame of this beam) can be determined from the momentum conservation law for the central plane wave Fourier harmonics of incident and reflected beams. (Because non-central Fourier harmonics of the beam at SF are generated by the non-central Fourier harmonics of the fundamental beams, and they also (as in the fundamental beams) constitute small angles with the direction of propagation of the signal beam.) Thus, the orientation of the reference frame associated with the reflected signal beam is given by the angle of reflection:

$$\sin\theta_3 = (\omega_1^2\sin^2\theta_1 + \omega_2^2\sin^2\theta_2 + 2\omega_1\omega_2\sin\theta_1\sin\theta_2\cos\alpha_2)^{1/2}/(\omega_1 + \omega_2) \quad (5)$$

between the perpendicular to the surface and the axis of the beam, and by the angle

$$\sin\alpha_3 = \omega_2\sin\theta_2\sin\alpha_2/\left[(\omega_1 + \omega_2)\sin\theta_3\right] \quad (6)$$

between the plane of reflection and the $x^{\Pi}z^{\Pi}$ plane of the surface reference frame (these angles are shown in figure 1).

Finally, we perform a reverse Fourier transform and obtain the desirable formula for the spatial distribution of an electric field in the cross section of the beam at SF ($\omega_3 = \omega_1 + \omega_2$) in its 'own' reference frame xyz:

$$\mathbf{E}_{3\perp}(x, y, z, t) = I_{\mathrm{F}}(x, y, z) \cdot \mathrm{e}^{-\mathrm{i}\omega_3 t + \mathrm{i}k_3^r z}[a_{3x}\mathbf{e}_x + a_{3y}\mathbf{e}_y + (a_{3xx}(z)x + a_{3yx}(z)y)\mathbf{e}_x + (a_{3xy}(z)x + a_{3yy}(z)y)\mathbf{e}_y] \tag{7}$$

where

$$I_{\mathrm{F}}(x, y, z) = \frac{\pi^2 E_{01} E_{02} w_1^2 w_2^2}{\sqrt{D_0 D_0'(z)}} \times \exp\left\{\frac{-h_x(z)x^2 - h_y(z)y^2 + 2h_{xy}xy}{D_0'(z)}\right\} \tag{8}$$

where, in its turn,

$$D_0 = \frac{w_1^4}{\cos^2\theta_1} + \frac{w_2^4}{\cos^2\theta_2} + w_1^2 w_2^2\left(\frac{1}{\cos^2\theta_1} + \frac{1}{\cos^2\theta_2} + \tan^2\theta_1 \tan^2\theta_2 \sin^2\alpha_2\right) \tag{9}$$

$$h_x(z) = \frac{w_1^2 w_2^2}{D_0}\left\{\frac{w_1^2[1 + \sin^2(\alpha_3 - \alpha_2)\tan^2\theta_2]}{\cos^2\theta_1} + \frac{w_2^2[1 + \sin^2\alpha_3 \cdot \tan^2\theta_1]}{\cos^2\theta_2}\right\} + \frac{2\mathrm{i}z}{k_3^r} \tag{10}$$

$$h_y(z) = \frac{w_1^2 w_2^2 \cos^2\theta_3}{D_0}\left\{\frac{w_1^2[1 + \cos^2(\alpha_3 - \alpha_2)\tan^2\theta_2]}{\cos^2\theta_1} + \frac{w_2^2[1 + \cos^2\alpha_3 \tan^2\theta_1]}{\cos^2\theta_2}\right\} + \frac{2\mathrm{i}z}{k_3^r} \tag{11}$$

$$h_{xy} = \frac{\cos\theta_3 w_1^2 w_2^2}{2D_0 \cos^2\theta_1 \cos^2\theta_2} \times (w_1^2 \sin 2(\alpha_3 - \alpha_2)\sin^2\theta_2 + w_2^2 \sin 2\alpha_3 \sin^2\theta_1) \tag{12}$$

$$D_0'(z) = \frac{w_1^4 w_2^4 \cos^2\theta_3}{D_0^2 \cos^2\theta_1 \cos^2\theta_2} \times \left[\frac{w_1^4}{\cos^2\theta_1} + \frac{w_2^4}{\cos^2\theta_2} + w_1^2 w_2^2 \tan^2\theta_1 \tan^2\theta_2 \sin^2\alpha_2\right] - 4z^2/(k_3^r)^2 + (2\mathrm{i}z/k_3^r)[h_x(0) + h_y(0)]. \tag{13}$$

Here $k_3^r = \omega_3/c$. It is worth remarking that (10) and (11) are the linear functions of z, and (13) is the quadratic polynomial one. Coefficients $a_{3x,y}$ are proportional to the zero order of the divergence angle of the beam, and they depend on the geometry of interaction of the incident beams, on their polarization states, on the linear and nonlinear optical susceptibilities of the medium bulk and surface. Coefficients $a_{3xx}(z)$, $a_{3yx}(z)$, $a_{3xy}(z)$ and $a_{3yy}(z)$ are proportional to the first order of the divergence angle of the beam. They also depend on all the above-mentioned values, and moreover the expressions for these coefficients include quantities (9)–(13) (i.e. they depend on the propagation coordinate z and on the effective sizes of the beam waists $w_{1,2}$). Because the expressions for both types of coefficients $a_{3x,y}$ and $a_{3xx}(z)$, $a_{3yx}(z)$, $a_{3xy}(z)$, $a_{3yy}(z)$ are very cumbersome, they are presented in the appendix of this paper.

4. The discussion of the obtained formulae. Analysis of the transversal distribution of the light field in the beam at sum-frequency

Before consideration of the new effects, it is necessary to remark that in the limiting case of the plane wave approximation ($w_m \to \infty$) for $\alpha_2 = 0$ the expression (7) is completely analogous to the result of [17]. Considering the particular case of second-harmonic generation and the normal incidence of the pump beam, we obtain the results of [27, 28], thoroughly studied there.

It follows from (7) and (8) that the transversal intensity distribution in the beam at SF is the product of the elliptic Gaussian distribution and the quadratic polynomial function of the coordinates x and y. At first, let us consider the part of the signal having zero order on the divergence angles of the beams, i.e. the elliptic Gaussian distribution with uniform distribution of the polarization state (determined by the coefficients $a_{3x,y}$). It is necessary to remark here that the plane wave approximation is not able to provide any information on the transversal intensity distribution even in the zero order on the divergence angle of the beam.

The ellipticity degree of the ellipses of equal intensity and the orientation of these ellipses do not depend on the polarization of incident beams and the nonlinear susceptibilities of the medium and its surface. These parameters of the intensity distribution are determined by the geometry of interaction of the incident beams and by the ratios of their frequencies and of their waists. They can be found directly from the exponential index in (8). The angle between one of the main axes of the ellipses of equal intensity and the x axis of the beam reference frame does not depend on the propagation coordinate (that is, the beam is not the rotating one):

$$\alpha = \frac{1}{2}\arctan\left\{\frac{2h_{xy}}{h_y(0) - h_x(0)}\right\}. \tag{14}$$

The ratio of the semi-axes of the ellipses of equal intensity is the following:

$$\frac{a(z)}{b(z)} = \frac{h_x(z)\sin^2\alpha + h_y(z)\cos^2\alpha + 2h_{xy}\sin\alpha\cos\alpha}{h_x(z)\cos^2\alpha + h_y(z)\sin^2\alpha - 2h_{xy}\sin\alpha\cos\alpha}. \tag{15}$$

Here the semi-axis $a(z)$ constitutes the angle α with the x axis and the semi-axis $b(z)$ is perpendicular to $a(z)$. In order to describe the ellipticity degree of the intensity distribution, it is more convenient to use and to analyze

$$M_{\mathrm{G}}(z) = 2\,[a(z)/b(z) + b(z)/a(z)]^{-1} \tag{16}$$

because $0 \leqslant M_{\mathrm{G}}(z) \leqslant 1$ even if $a(z)/b(z) \to \infty$ or $a(z)/b(z) \to 0$. If the ellipse tends to collapse and its shape is close to a line, then $M_{\mathrm{G}}(z) \to 0$. If the ellipse turns into a circle, then $M_{\mathrm{G}}(z) = 1$.

Characteristic dependences of α and $M_{\mathrm{G}}(z = 0)$ on the angle of incidence θ_1 for different values of α_2 and for two values of w_2/w_1 are shown in figure 2. Both the orientation and the shape of the ellipses of equal intensity are changing within the relatively broad range, depending on the geometry

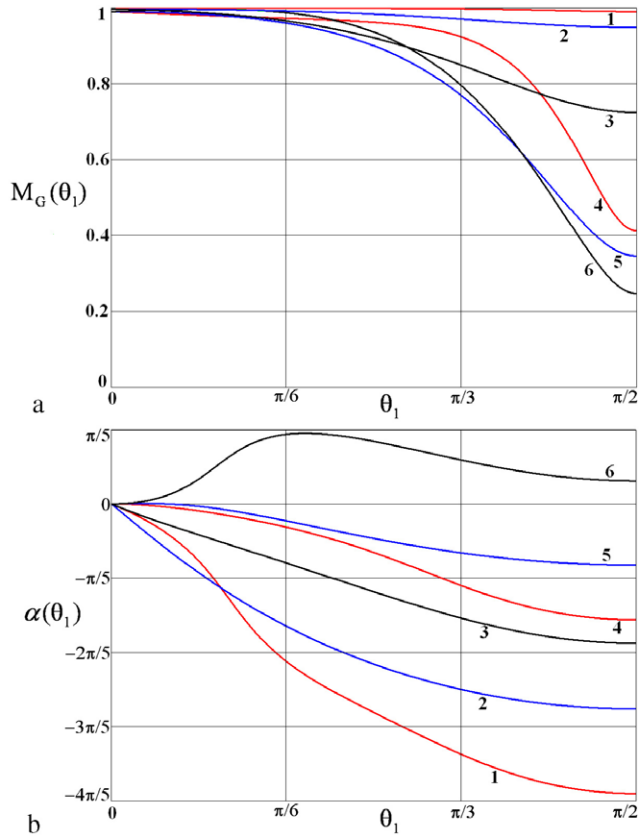

Figure 2. Dependences of the ellipticity degree $M_G(\theta_1, z = 0)$ (a) and the rotation angle $\alpha(\theta_1)$ (b) of the elliptic Gaussian intensity distribution; $\theta_2 = 60°$; curves **1** and **4** correspond to $\alpha_2 = 30°$; **2** and **5** correspond to $\alpha_2 = 90°$; **3** and **6** correspond to $\alpha_2 = 150°$. For **1**, **2** and **3** $w_2/w_1 = 1$; for **4**, **5** and **6** $w_2/w_1 = 5$.

of interaction and ratio of the waists of the incident beams even if the beams are not tightly focused. The range of variation of α and $M_G(z = 0)$ grows with the increase of any of the angles of incidence. If one of the angles is equal to zero (for example, $\theta_1 = 0$) there appears a symmetry plane in this task, coinciding with the plane of incidence of the other beam. In this case, the intensity distribution is also symmetric relative to this plane and this means that $\alpha(\theta_1 = 0) = \alpha(\theta_2 = 0) = 0$, and that the ellipticity degree $M_G(z)$ does not depend on α_2. This fact can also be seen from figure 2 (and it follows from (14) and (15)).

Now let us include into the consideration the first-order (on the divergence angle) terms in (7). It can be shown that the effective transversal size of the SF beam is of the order of $w_{SF} = w_1 w_2/\sqrt{w_1^2+w_2^2}$. The order of the latter quantity is the same as for $w_{1,2}$, when these values are of the same order ($w_1 \sim w_2$). Otherwise, if $w_1 \gg w_2$ or $w_2 \gg w_1$, the w_{SF} is of the order of $\min(w_1, w_2)$. (It is worth noticing that in the case of normal incidence of both beams ($\theta_{1,2} = 0$) the effective transversal size of the signal beam is equal to w_{SF}.) Thus, due to the exponential index in (8), the amplitude of the signal at SF tends to zero if $x \gg w_{SF}$ or $y \gg w_{SF}$ and we should consider $x, y \sim w_{SF}$ or $x, y < w_{SF}$ in order to deal with the amplitude of the signal significantly distinguishable from zero.

The divergence angles of the fundamental beams of Gaussian profiles are approximately equal to $\lambda_{1,2}/(\pi w_{1,2})$ (this appreciation is true for small angles). It can be shown (by estimation of the expressions (A.1), (A.2), (A.7) and (A.8) in the appendix) that, if $x, y \sim w_{SF}$, the ratios like $a_{3ij}(z)x/a_{3i}$ ($i, j = x, y$) are of the order of $\max(\lambda_1/(\pi w_1), \lambda_2/(\pi w_2))$. If (as it usually takes place) the rest of the quantities in the coefficients $a_{3ij}(z)$ and a_{3i} make contributions of approximately the same order, then, for $w_{1,2}/\lambda_{1,2} \geqslant 10$, the non-Gaussian part of the field will be much less than the Gaussian one. In this case it will act as a weak distortion of the uniformly polarized elliptic Gaussian beam at SF. Such a situation is illustrated in figure 3. The intensity distribution in the cross section of the beam at SF shown in figure 3(a) is elliptic Gaussian. The intensity in the figure is a normalized quantity $I(x, y) = \frac{\sqrt{D_0 D_0'(0)}}{\pi^2 E_{01} E_{02} w_1^2 w_2^2 \kappa_{zxx}^{(2)}} |\mathbf{E}_{3\perp}(x, y, 0, t)|^2$ for $z = 0$ in normalized coordinates x/w_{SF} and y/w_{SF}. Of course, the signal is usually measured at some distance from the surface of the medium, but we consider the simplest case in order to avoid additional complexity, connected with the parabolic increase of the oscillation phase during the propagation of the beam in free space. Thus, we aim to demonstrate the main features of the SF signal and of the transversal distributions of its intensity and polarization. Figure 3(b) illustrates the polarization distribution in the cross section of the reflected beam. The ellipses in the figure show the polarization ellipses in the corresponding points of the SF beam cross section. The sum of squared axes of each ellipse is proportional to the intensity of light at the point indicated by the ellipse. The ellipticity degree and the angle of the orientation of the ellipses in the figure correspond to the same characteristics of the polarization ellipses. The spots at the contours of the ellipses indicate the direction of the electric field vector at fixed timing at $t = k_3^r z/\omega_3$ (from the center of the ellipse to such a spot). As can be seen from figure 3(b), the polarization is practically uniformly distributed in the beam cross section, and it does not change significantly during the propagation of the beam.

Let us now focus our attention on the question, whether the first-order non-Gaussian part of the field is able to affect significantly the structure of the beam at SF (apart from the case of normal incidence of the pump beams)?

The analysis of the coefficients $a_{3ij}(z)$, a_{3i} ($i, j = x, y$) have shown that, in typical cases, their dependence on the medium parameters, on the polarization of the fundamental beams and their waists is not able to change the order of their ratio. But the dependences of $a_{3ij}(z)$ and a_{3i} on the angles of incidence θ_1 and θ_2 are different. If we suppose that θ_1 and/or θ_2 are tending to 90° in such a way that $\cos\theta_1$ and/or $\cos\theta_2$ become small, then $a_{3ij}(z) \sim \cos\theta_1/\cos\theta_2 + \cos\theta_2/\cos\theta_1$ and $a_{3i} \sim \cos\theta_1 \cos\theta_2$. Thus, in this case $a_{3ij}(z)w_{SF}/a_{3i} \sim (1/\cos^2\theta_1 + 1/\cos^2\theta_2)\lambda_{1,2}/(\pi w_{1,2})$. If we make our appreciations for $w_{1,2}/\lambda_{1,2} = 10$ and $\theta_{1,2} \geqslant 80°$, then it appears that $|a_{3ij}(z)w_{SF}/a_{3i}| > 1$, and the contribution of the non-Gaussian part of the field in this case will seriously affect the structure of the beam. This situation is very clear in figure 4, where the distributions of intensity and of the polarization are shown for the case when one of the angles of incidence is large enough ($\theta_1 = 82°$). The intensity distribution in figure 4(a) has several local extrema and significantly differs from the Gaussian one, though the

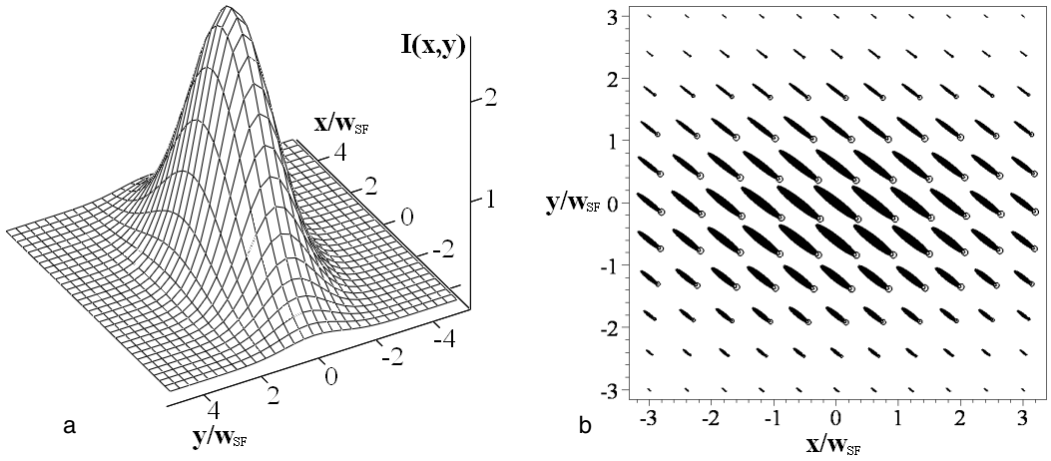

Figure 3. The transversal distribution of the intensity (a) and of the polarization (b) in a sum-frequency beam. The intensity distribution is elliptic Gaussian and the polarization almost does not change along the beam cross section. $w_2/w_1 = 0.7$, $\omega_2/\omega_1 = 1.5$, $\alpha_2 = 180°$, $\theta_1 = \theta_2 = 60°$, $M_{01} = -0.5$, $M_{02} = 0.8$, $\Psi_1 = 60°$, $\Psi_2 = -30°$; $n_1 = 1.26$, $n_2 = 1.3$, $n_3 = 1.34$; $b_2/b_1 = 1.2$, $b_3/b_1 = 1$, $b_4/b_1 = 1.1$, $b_5/b_1 = 2$, $b_6/b_1 = -2.2$, $b_7/b_1 = 0.6$, $\gamma_1/b_1 = 1.2$, $\gamma_2/b_1 = 0.8$, $\gamma_3/b_1 = 1.4$, $\gamma_4/b_1 = 0.5$, $\chi/b_1 = 1$.

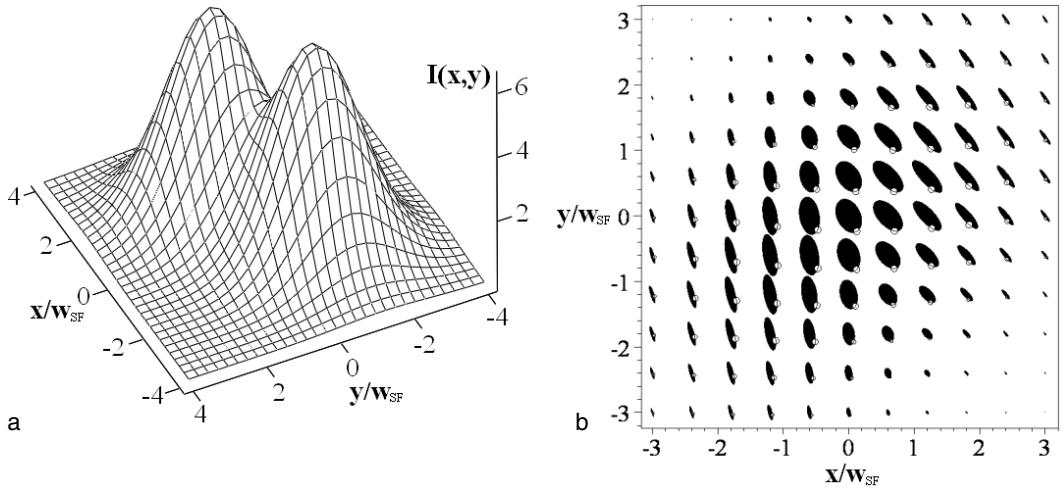

Figure 4. The transversal distribution of the intensity (a) and of the polarization (b) in sum-frequency beam, when $\theta_1 = 82°$, $\theta_2 = 30°$. The intensity distribution has non-Gaussian shape and the polarization significantly changes along the beam cross section. $w_2/w_1 = 1$, $\omega_2/\omega_1 = 1.5$, $\alpha_2 = 90°$, $M_{01} = -0.4$, $M_{02} = 0.8$, $\Psi_1 = 0$, $\Psi_2 = 90°$; $n_1 = 1.26$, $n_2 = 1.3$, $n_3 = 1.34$; $b_2/b_1 = 1.2$, $b_3/b_1 = 0.5$, $b_4/b_1 = 0.3$, $b_5/b_1 = 2$, $b_6/b_1 = -2.2$, $b_7/b_1 = 0.6$, $\gamma_1/b_1 = 1.2$, $\gamma_2/b_1 = 0.8$, $\gamma_3/b_1 = 1.4$, $\gamma_4/b_1 = 0.5$, $\chi/b_1 = 0.8$.

divergence angles of the pump beams are small (about 2°–3°). Moreover, they are several times smaller than the angle between the direction of propagation of the first beam and the surface of the medium ($90° - \theta_1 = 8°$). As can be seen from figure 4(b), the polarization distribution in such cases becomes strongly inhomogeneous and the parameters of the polarization ellipses of the light can differ significantly along the cross section of the signal beam.

Generally, the exact values of the angles of incidence, making the non-Gaussian part of the field of the order of the Gaussian one, depend not only on the focusing of the incident beams (the size of their waists). The values of these angles may vary for about several degrees, conditioned by the values of the other parameters of incident radiation and the medium. We emphasize that for a non-Gaussian part of the field in order to be comparable with the Gaussian part, it is enough for $\cos^2\theta_{1,2}$ to be a small value (not necessary for $\cos\theta_{1,2}$ itself). In certain cases such a condition can be satisfied even for relatively moderate values of $\theta_{1,2} < 80°$. In addition, in special cases, relations between the medium parameters and/or geometry of incidence may provide the disappearance of the response of the medium of zero order on the divergence angles (or, at least, these relations may make this response small enough). In such a case this effect will not be connected directly with the values of $\theta_{1,2}$. But such situations can hardly be described by certain mathematical expressions in this task, and usually they are not practically important.

The overall dependence of the transversal distribution of the polarization in the signal beam on the components of the tensors $\chi^{(2)}_{ijk}$, $\gamma^{(2)}_{ijkl}$ and $\kappa^{(2)}_{ijk}$ is very complicated and a complete description of this dependence is given in the appendix. Generally, the expression for the electric field at SF (7) contains

various linear combinations of all of the components of these tensors with complex coefficients. These coefficients depend on the geometry of incidence, polarization, frequencies and waists of the incident beams, and on the refraction indexes of the medium.

5. Conclusion

In our work we have obtained the analytical formula completely describing the transversal spatial distribution of the electric field in a light beam at sum-frequency generated from the surface of an isotropic chiral medium by elliptically polarized Gaussian beams at fundamental frequencies. This formula was examined and conclusions were found on the limitations of the applicability of the plane wave approximation in this task. We have also studied the transversal structure of the signal beam at sum-frequency for the arbitrary geometry of the incidence of the fundamental beams.

It was established that in typical cases the intensity distribution in the cross section of the signal beam is elliptic Gaussian, and its shape (the ellipticity and the orientation) significantly varies, depending on the geometry of the incidence of the fundamental beams. In such cases the non-Gaussian part of the field (which is always present in the reflected beam at sum-frequency) is weak, compared with the Gaussian one, and it introduces only small distortions in the transversal distributions of the polarization and intensity.

However, for large values of at least one of the angles of incidence of the pump beams (as a rule, $\geqslant 80°$) this non-Gaussian part becomes comparable with the Gaussian one (or even exceeds it). In such a case the intensity distribution is more complicated and the polarization state of light significantly changes along the beam cross section.

The knowledge about the features of the distribution of the electric field vector in cross section of the beam at sum-frequency provides the possibility of correct interpretation of the experimentally measured mean value of polarization of the signal beam. Also, as was shown in earlier work [28], the studies of the transversal distribution of light polarization in a signal beam provide additional information on the properties of the investigated medium, which is very helpful in modern problems of diagnostics, spectroscopy and characterization of chiral materials. In particular, the three-wave mixing methods can be useful for characterization of quadratic optical susceptibilities of chiral metamaterials, which are able to provide a prominent quadratic optical response even in the case of surface interaction of the incident waves.

Appendix

The coefficients $a_{3x,y}$ in (7) are given by the following expressions:

$$a_{3x} = \frac{4\pi[\cos\theta_3' \cdot (\mathbf{S}_\perp^{(0)} \cdot \mathbf{e}_{\alpha 3}^\Pi) + \sin\theta_3' \cdot S_z^{(0)}]}{\cos\theta_3' + n_3\cos\theta_3} \tag{A.1}$$

$$a_{3y} = \frac{4\pi([\mathbf{S}_\perp^{(0)} \times \mathbf{e}_{\alpha 3}^\Pi] \cdot \mathbf{e}_z^\Pi)}{n_3\cos\theta_3' + \cos\theta_3}. \tag{A.2}$$

Here n_3 is the refraction index of the medium at frequency $\omega_3 = \omega_1 + \omega_2$, θ_3' is the angle of refraction of the beam at sum-frequency (the angle determined from the momentum conservation law and the refraction of the central Fourier harmonic of the refracted beam at SF), $\sin\theta_3' = \sin\theta_3/n_3$, $\mathbf{e}_{\alpha 3}^\Pi$ is the unit vector within the plane $x^\Pi y^\Pi$ (plane of the surface) in the direction of the sum-frequency beam (constituting the angle α_3 with x^Π axis), $\mathbf{e}_{\alpha 3}^\Pi = \mathbf{e}_x^\Pi\cos\alpha_3 + \mathbf{e}_y^\Pi\sin\alpha_3$, where the vectors $\mathbf{e}_{x,y,z}^\Pi$ are the unit vectors of the surface reference frame $x^\Pi y^\Pi z^\Pi$. Vector $\mathbf{S}^{(0)}$ is defined in the surface reference frame $x^\Pi y^\Pi z^\Pi$ and it contains a zero-order part (on the divergence angle) of the nonlinear polarization and nonlinear current density. $\mathbf{S}_\perp^{(0)}$ is the component of this vector, lying in $x^\Pi y^\Pi$, $\mathbf{S}^{(0)} = \mathbf{S}_\perp^{(0)} + S_z^{(0)}\mathbf{e}_z^\Pi = S_x^{(0)}\mathbf{e}_x^\Pi + S_y^{(0)}\mathbf{e}_y^\Pi + S_z^{(0)}\mathbf{e}_z^\Pi$. The vector is defined as follows:

$$\mathbf{S}^{(0)} = \frac{1}{c}(\mathbf{i}_\perp^{(0)} + n_3^2 i_z^{(0)}\mathbf{e}_z^\Pi) + \frac{\omega_3}{n_3\omega_3\cos\theta_3' + n_1\omega_1\cos\theta_1' + n_2\omega_2\cos\theta_2'}\mathbf{P}^{(0)}. \tag{A.3}$$

Angles $\theta_{1,2}'$ are the angles of refraction of the incident beams, $\sin\theta_{1,2}' = \sin\theta_{1,2}/n_{1,2}$, where $n_{1,2}$ are the refraction indexes at $\omega_{1,2}$. In (A.3) $\mathbf{i}_\perp^{(0)} = i_x^{(0)}\mathbf{e}_x^\Pi + i_y^{(0)}\mathbf{e}_y^\Pi$. The zero-order parts of the nonlinear polarization and the nonlinear current density are given by the following expressions:

$$\begin{aligned}
i_x^{(0)} &= -b_3a_{1x}a_{2z} - b_4a_{1z}a_{2x}^\Pi - b_5a_{1y}a_{2z} + b_6a_{1z}a_{2y}^\Pi \\
i_y^{(0)} &= -b_3a_{1y}a_{2z} - b_4a_{1z}a_{2y}^\Pi + b_5a_{1x}a_{2z} - b_6a_{1z}a_{2x}^\Pi \\
i_z^{(0)} &= b_7[a_{1y}a_{2x}^\Pi - a_{1x}a_{2y}^\Pi] - b_2a_{1z}a_{2z} - b_1[a_{1x}a_{2x}^\Pi + a_{1y}a_{2y}^\Pi]
\end{aligned} \tag{A.4}$$

$$\begin{aligned}
\mathbf{P}^{(0)} = \frac{1}{c}\big(&\mathbf{e}_x^\Pi\big\{\chi[-a_{1y}a_{2z}/n_2^2 + a_{2y}^\Pi a_{1z}/n_1^2] \\
&+ \mathrm{i}[a_{1x}a_{2x}^\Pi + a_{1y}a_{2y}^\Pi + a_{1z}a_{2z}/n_1^2n_2^2] \\
&\times [(\omega_1/\omega_3)\gamma_1\sin\theta_1 + (\omega_2/\omega_3)\gamma_2\sin\theta_2\cos\alpha_2] \\
&+ \mathrm{i}\,\gamma_3a_{1x}(\omega_1/\omega_3)[a_{2x}^\Pi\sin\theta_1 - a_{2z}n_1\cos\theta_1'/n_2^2] \\
&+ \mathrm{i}\gamma_4(\omega_2/\omega_3)a_{2x}^\Pi[a_{1x}\sin\theta_2\cos\alpha_2 + a_{1y}\sin\theta_2\sin\alpha_2 \\
&- a_{1z}n_2\cos\theta_2'/n_1^2]\big\} + \mathbf{e}_y^\Pi\big\{\chi[a_{2z}a_{1x}/n_2^2 - a_{1z}a_{2x}^\Pi/n_1^2] \\
&+ \mathrm{i}\gamma_2(\omega_2/\omega_3)\times\sin\theta_2\sin\alpha_2 \\
&\times [a_{1x}a_{2x}^\Pi + a_{1y}a_{2y}^\Pi + a_{1z}a_{2z}/n_1^2n_2^2] \\
&+ \mathrm{i}\gamma_3(\omega_1/\omega_3)a_{1y}[a_{2x}^\Pi\sin\theta_1 - a_{2z}n_1\cos\theta_1'/n_2^2] \\
&+ \mathrm{i}\gamma_4(\omega_2/\omega_3)a_{2y}^\Pi[a_{1x}\sin\theta_2\cos\alpha_2 + a_{1y}\sin\theta_2\sin\alpha_2 \\
&- a_{1z}n_2\cos\theta_2'/n_1^2]\big\} + \mathbf{e}_z^\Pi\{\chi[a_{1x}a_{2y}^\Pi - a_{1y}a_{2x}^\Pi] \\
&+ \mathrm{i}[a_{1x}a_{2x}^\Pi + a_{1y}a_{2y}^\Pi + a_{1z}a_{2z}/n_1^2n_2^2] \\
&\times [n_1(\omega_1/\omega_3)\gamma_1\cos\theta_1' + n_2(\omega_2/\omega_3)\gamma_2\cos\theta_2'] \\
&- \mathrm{i}\gamma_3(\omega_1/\omega_3)a_{1z}[a_{2x}^\Pi\sin\theta_1 - n_1a_{2z}\cos\theta_1'/n_2^2]/n_1^2 \\
&- \mathrm{i}\gamma_4(\omega_2/\omega_3)a_{2z}[a_{1x}\sin\theta_2\cos\alpha_2 \\
&+ a_{1y}\sin\theta_2\sin\alpha_2 - a_{1z}n_2\cos\theta_2'/n_1^2]/n_2^2\}\big).
\end{aligned} \tag{A.5}$$

In (A.4) the quantities $b_{1,\ldots,7}$ are 7 independent non-zero components of the tensor of the quadratic optical response of the medium surface $\kappa_{ijk}^{(2)}$; the structure of this tensor is determined by the symmetry group ∞ of the surface of the chiral medium: $b_1 = \kappa_{zxx}^{(2)} = \kappa_{zyy}^{(2)}$, $b_2 = \kappa_{zzz}^{(2)}$, $b_3 = \kappa_{yyz}^{(2)} = \kappa_{xxz}^{(2)}$, $b_4 = \kappa_{yzy}^{(2)} = \kappa_{xzx}^{(2)}$, $b_5 = \kappa_{xyz}^{(2)} = -\kappa_{yxz}^{(2)}$, $b_6 = -\kappa_{xzy}^{(2)} = \kappa_{yzx}^{(2)}$, $b_7 = \kappa_{zxy}^{(2)} = -\kappa_{zyx}^{(2)}$.

In (A.5) $\chi = c \cdot \chi^{(2)}_{xyz}$ is proportional to the single non-zero component of the tensor $\chi^{(2)}_{ijk}$ of the local quadratic optical response of the bulk of the isotropic chiral medium; $\gamma_{1,2} = \omega_3 \gamma^{(2)\,1,2}_{xxyy}$, $\gamma_3 = \omega_3 \gamma^{(2)\,1}_{xyxy}$, $\gamma_4 = \omega_3 \gamma^{(2)\,2}_{xyyx}$ are the components of the tensor of the spatial dispersion of the quadratic optical response of the bulk of this medium. Coefficients a_{mi}, a_{mij} and a^{Π}_{mij} in (A.4) and (A.5) (where $m = 1,\ 2$; $i = x, y, z$; $j = x, y$) are defined as follows:

$$a_{my} = \frac{2\cos\theta_m e_{my}}{n_m \cos\theta'_m + \cos\theta_m}$$

$$a_{mx} = \frac{2\cos\theta_m \cos\theta'_m e_{mx}}{n_m \cos\theta_m + \cos\theta'_m}$$

$$a_{myy} = \frac{\sin\theta_m \cdot (n_m^2 - 1)}{n_m(n_m\cos\theta_m + \cos\theta'_m)} \cdot \frac{2\cos\theta_m e_{mx}}{n_m\cos\theta'_m + \cos\theta_m}$$

$$\begin{aligned} a_{mxx} = {} & \frac{2\cos\theta_m e_{mx}}{n_m\cos\theta'_m + \cos\theta_m} \\ & \times \left[-\mathrm{tg}\,\theta_m + \frac{n_m^2 - 1}{n_m(n_m\cos\theta_m + \cos\theta'_m)} \right. \\ & \times \left(2\sin\theta_m + \frac{(n_m^2\,\mathrm{tg}\,\theta_m + \mathrm{tg}\,\theta'_m)\sin^2\theta_m}{n_m(n_m\cos\theta_m + \cos\theta'_m)} \right) \\ & + \frac{(1 - n_m^2)\mathrm{tg}\,\theta'_m}{(n_m\cos\theta'_m + \cos\theta_m)\cos^2\theta_m} \\ & \left. \times \left(\cos\theta_m + \frac{(n_m^2 - 1)\sin^2\theta_m}{n_m(n_m\cos\theta_m + \cos\theta'_m)} \right) \right] \end{aligned}$$

$$a_{mxy} = a_{my}\frac{(1 - n_m^2)\mathrm{tg}\,\theta'_m}{(n_m\cos\theta'_m + \cos\theta_m)\cos^2\theta_m}$$

$$a_{myx} = -a_{my}\frac{(n_m\cos\theta'_m + \cos\theta_m)\sin\theta_m}{n_m(n_m\cos\theta_m + \cos\theta'_m)}$$

$$a_{mz} = a_{mx}\mathrm{tg}\,\theta'_m n_m^2$$

$$a_{1zx} = a_{1xx}\mathrm{tg}\,\theta'_1 n_1^2 + \frac{n_1 a_{1x}}{\cos^3\theta'_1}$$

$$a_{1zy} = a_{1yx}\mathrm{tg}\,\theta'_1 n_1^2 + \frac{n_1 a_{1y}}{\cos\theta'_1}$$

$$\begin{aligned} a_{2zx} = {} & (a_{2xx}\cos\alpha_2 - a_{2yx}\sin\alpha_2)\mathrm{tg}\,\theta'_2 n_2^2 \\ & + \frac{n_2(a_{2x}\cos\alpha_2 - a_{2y}\cos^2\theta'_2\sin\alpha_2)}{\cos^3\theta'_2} \end{aligned}$$

$$\begin{aligned} a_{2zy} = {} & (a_{2xx}\sin\alpha_2 + a_{2yx}\cos\alpha_2)\mathrm{tg}\,\theta'_2 n_2^2 \\ & + \frac{n_2(a_{2x}\sin\alpha_2 - a_{2y}\cos^2\theta'_2\cos\alpha_2)}{\cos^3\theta'_2} \end{aligned}$$

$$a^{\Pi}_{2x} = a_{2x}\cos\alpha_2 - a_{2y}\sin\alpha_2$$

$$a^{\Pi}_{2y} = a_{2y}\cos\alpha_2 + a_{2x}\sin\alpha_2$$

$$\begin{aligned} a^{\Pi}_{2xx} = {} & -(a_{2yx} + a_{2xy})\cos\alpha_2\sin\alpha_2 \\ & + a_{2xx}\cos^2\alpha_2 + a_{2yy}\sin^2\alpha_2 \end{aligned}$$

$$\begin{aligned} a^{\Pi}_{2yx} = {} & (a_{2xx} - a_{2yy})\cos\alpha_2\sin\alpha_2 \\ & + a_{2yx}\cos^2\alpha_2 - a_{2xy}\sin^2\alpha_2 \end{aligned}$$

$$\begin{aligned} a^{\Pi}_{2xy} = {} & (a_{2xx} - a_{2yy})\cos\alpha_2\sin\alpha_2 \\ & - a_{2yx}\sin^2\alpha_2 + a_{2xy}\cos^2\alpha_2 \end{aligned}$$

$$\begin{aligned} a^{\Pi}_{2yy} = {} & (a_{2yx} + a_{2xy})\cos\alpha_2\sin\alpha_2 \\ & + a_{2xx}\sin^2\alpha_2 + a_{2yy}\cos^2\alpha_2. \end{aligned} \tag{A.6}$$

Coefficients $a_{3jx}(z)$, $a_{3jy}(z)$ ($j = x, y$), describing the quantities of the first order on the divergence angle of the beam in (7) are more complex, than $a_{3x,y}$:

$$\begin{aligned} a_{3jx}(z) = {} & \frac{4\pi\cos\theta'_3(\mathbf{S}^{(j)}_{\perp}(z)\cdot\mathbf{e}^{\Pi}_{\alpha 3})}{\cos\theta'_3 + n_3\cos\theta_3} - \frac{4\pi(\mathbf{S}^{(0)}_{\perp}\cdot\mathbf{e}^{\Pi}_{\alpha 3})g^{(j)}(z)}{k^r_3\cos\theta_3} \\ & \times \left[\frac{\tan\theta_3 - \tan\theta'_3}{(n_3\cos\theta'_3 + \cos\theta_3)^2} + \sin^2\theta'_3\frac{\tan\theta'_3 - n_3^2\tan\theta_3}{(\cos\theta'_3 + n_3\cos\theta_3)^2} \right. \\ & \left. + \frac{\sin^2\theta_3\cos\theta'_3\tan\theta_3}{\cos\theta'_3 + n_3\cos\theta_3} + \frac{(1 + \sin^2\theta_3)\sin\theta'_3}{\cos\theta'_3 + n_3\cos\theta_3} \right] \\ & - (\mathbf{f}^{(j)}(z)\cdot\mathbf{S}^{(0)}_{\perp}) \\ & \times \frac{4\pi(1 - n_3^2)\sin\theta'_3}{k^r_3(\cos\theta'_3 + n_3\cos\theta_3)(n_3\cos\theta'_3 + \cos\theta_3)} \\ & + S^{(j)}_z(z) \times \frac{4\pi\sin\theta'_3}{\cos\theta'_3 + n_3\cos\theta_3} \\ & + \frac{4\pi S^{(0)}_z g^{(j)}(z)}{k^r_3 n_3(\cos\theta'_3 + n_3\cos\theta_3)} \left[1 + \sin^2\theta_3 + (n_3\cos^2\theta'_3 \right. \\ & \times \sin\theta_3 + \sin\theta'_3 - n_3^2\cos\theta'_3\tan\theta_3\sin^2\theta_3) \\ & \left. \times \frac{\tan\theta'_3}{\cos\theta'_3 + n_3\cos\theta_3} \right] \\ & + \frac{4\pi(\tan\theta^{\mathrm{P}}_3 + \tan\theta'_3)\omega_3^2 g^{(j)}(z)}{(n_3\omega_3\cos\theta'_3 + n_1\omega_1\cos\theta'_1 + n_2\omega_2\cos\theta'_2)^2 k^r_3\cos\theta_3} \\ & \times \left[P^{(0)}_z \times \frac{\cos\theta_3\sin\theta'_3}{\cos\theta'_3 + n_3\cos\theta_3} \right. \\ & \left. + (\mathbf{P}^{(0)}_{\perp}\cdot\mathbf{e}^{\Pi}_{\alpha 3})\frac{\cos\theta'_3\cos^2\theta_3 + n_3\cos\theta_3\cos^2\theta'_3}{(\cos\theta'_3 + n_3\cos\theta)(n_3\cos\theta'_3 + \cos\theta_3)} \right] \end{aligned} \tag{A.7}$$

$$\begin{aligned} a_{3jy}(z) = {} & -\frac{4\pi}{n_3\cos\theta'_3 + \cos\theta_3} \\ & \times \left[(\mathbf{e}^{\Pi}_z\cdot[\mathbf{e}^{\Pi}_{\alpha 3}\times\mathbf{S}^{(j)}_{\perp}(z)]) - (\mathbf{e}^{\Pi}_z\cdot[\mathbf{e}^{\Pi}_{\alpha 3}\times\mathbf{S}^{(0)}_{\perp}]) \right. \\ & \left. \times g^{(j)}(z)\frac{\tan\theta_3 - \tan\theta'_3}{k^r_3(n_3\cos\theta'_3 + \cos\theta_3)} \right] \\ & + \frac{4\pi(\mathbf{e}^{\Pi}_z\cdot[\mathbf{e}^{\Pi}_{\alpha 3}\times\mathbf{f}^{(j)}(z)])}{k^r_3 n_3(\cos\theta'_3 + n_3\cos\theta_3)} \\ & \times [(\mathbf{e}^{\Pi}_{\alpha 3}\cdot\mathbf{S}^{(0)}_{\perp})\sin\theta_3 - S^{(0)}_z\cos\theta_3] \\ & - \frac{4\pi(\tan\theta^{\mathrm{P}}_3 + \tan\theta'_3)g^{(j)}(z)}{k^r_3(n_3\cos\theta'_3 + \cos\theta_3)} \\ & \times \frac{\omega_3^2(\mathbf{e}^{\Pi}_z\cdot[\mathbf{e}^{\Pi}_{\alpha 3}\times\mathbf{P}^{(0)}_{\perp}])}{(n_3\omega_3\cos\theta'_3 + n_1\omega_1\cos\theta'_1 + n_2\omega_2\cos\theta'_2)^2}. \end{aligned} \tag{A.8}$$

Here the angle θ^{P}_3 determines the propagation direction of the wave of medium polarization (inside the medium). It is determined by the expression

$$\begin{aligned} \sin\theta^{\mathrm{P}}_3 = {} & \{\omega_3\sin\theta_3\}\{((n_1\omega_1)^2 + (n_2\omega_2)^2 \\ & + 2n_1n_2\omega_1\omega_2(\cos\theta'_1\cos\theta'_2 + \sin\theta'_1\sin\theta'_2\cos\alpha_2))\}^{-1/2}. \end{aligned} \tag{A.9}$$

All the dependences on z are contained in the functions $g^{(j)}(z)$ and $\mathbf{f}^{(j)}(z)$, incorporated in all the other quantities, which depend on z (they also appear in $\mathbf{S}^{(j)}(z)$). These functions, in their turn, contain these dependences through the quantities $h_x(z)$ and $D_0'(z)$ given by the expressions (10) and (13) in the main body of the paper:

$$\begin{aligned} g^{(x)}(z) &= -[2\mathrm{i}/D_0'(z)]h_x(z)\cos\theta_3, \\ g^{(y)}(z) &= [2\mathrm{i}/D_0'(z)]h_{xy}\cos\theta_3, \\ \mathbf{f}^{(x)}(z) &= [2\mathrm{i}/D_0'(z)]h_{xy}[\mathbf{e}_z^{\Pi}\times\mathbf{e}_{\alpha 3}^{\Pi}] + g^{(x)}(z)\mathbf{e}_{\alpha 3}^{\Pi}, \\ \mathbf{f}^{(y)}(z) &= g^{(y)}(z)\mathbf{e}_{\alpha 3}^{\Pi} + 2\mathrm{i}\frac{D_0'(z)-h_{xy}^2}{D_0'(z)h_x(z)}[\mathbf{e}_z^{\Pi}\times\mathbf{e}_{\alpha 3}^{\Pi}]. \end{aligned} \tag{A.10}$$

The quantity $\mathbf{S}^{(j)}(z)$ is defined analogously to $\mathbf{S}^{(0)}$ and it contains the vectors $\mathbf{P}^{(j)}(z)$ and $\mathbf{i}^{(j)}(z)$, which are directly connected with the first-order parts of nonlinear polarization and nonlinear current density:

$$\begin{aligned} \mathbf{S}^{(j)}(z) &= \frac{1}{c}(\mathbf{i}_{\perp}^{(j)}(z) + n_3^2\mathrm{i}_z^{(j)}(z)\mathbf{e}_z^{\Pi}) \\ &\quad + \frac{\omega_3}{n_3\omega_3\cos\theta_3' + n_1\omega_1\cos\theta_1' + n_2\omega_2\cos\theta_2'}\mathbf{P}^{(j)}(z). \end{aligned} \tag{A.11}$$

These quantities $\mathbf{P}^{(j)}(z)$ and $\mathbf{i}^{(j)}(z)$ are coefficients before the coordinates in the corresponding linear coordinate dependences of the first-order parts of the nonlinear polarization and nonlinear current density (in the reference frame of the reflected beam). These coefficients (depending on z) are given by the following expressions:

$$\begin{aligned} \mathbf{i}^{(j)}(z) &= \mathbf{i}_{\perp}^{(j)}(z) + \mathrm{i}_z^{(j)}(z)\mathbf{e}_z^{\Pi} \\ &= \mathrm{i}_x^{(j)}(z)\mathbf{e}_x^{\Pi} + \mathrm{i}_y^{(j)}(z)\mathbf{e}_y^{\Pi} + \mathrm{i}_z^{(j)}(z)\mathbf{e}_z^{\Pi} \\ \mathbf{P}^{(j)}(z) &= \mathbf{P}_{\mathrm{loc}}^{(j)}(z) + \mathbf{P}_{\mathrm{nloc1}}^{(j)}(z) + \mathbf{P}_{\mathrm{nloc2}}^{(j)}(z) + \mathbf{P}_{\mathrm{nloc3}}^{(j)}(z). \end{aligned} \tag{A.12}$$

The corresponding constituents of (A.12) are given as follows:

$$\begin{aligned} \mathbf{P}_{\mathrm{loc}}^{(j)}(z) &= \chi_{xyz}^{(2)}\{[-(a_{2z}/n_2^2)A_{1y}^{(j)}(z) - (a_{1y}/n_2^2)A_{2x}^{(j)}(z) \\ &\quad + (a_{1z}/n_1^2)A_{2y}(z) + (a_{2y}^{\Pi}/n_1^2)A_{1z}^{(j)}(z)]\mathbf{e}_x^{\Pi} \\ &\quad + [-(a_{1z}/n_1^2)A_{2x}^{(j)}(z) - (a_{2x}^{\Pi}/n_1^2)A_{1z}^{(j)}(z) \\ &\quad + (a_{2z}/n_2^2)A_{1x}^{(j)}(z) + (a_{1x}/n_2^2)A_{2z}^{(j)}(z)]\mathbf{e}_y^{\Pi} \\ &\quad + [a_{1x}A_{2y}^{(j)}(z) + a_{2y}^{\Pi}A_{1x}^{(j)}(z) \\ &\quad - a_{1y}A_{2x}^{(j)}(z) - a_{2x}^{\Pi}A_{1y}^{(j)}(z)]\mathbf{e}_z^{\Pi}\} \end{aligned} \tag{A.13}$$

$$\begin{aligned} \mathbf{P}_{\mathrm{nloc1}}^{(j)}(z) &= (\mathrm{i}/c)\{[((\omega_1/\omega_3)\gamma_1\sin\theta_1 \\ &\quad + (\omega_2/\omega_3)\gamma_2\sin\theta_2\cos\alpha_2)\mathbf{e}_x^{\Pi} \\ &\quad + (\omega_2/\omega_3)\gamma_2\sin\theta_2\sin\alpha_2\mathbf{e}_y^{\Pi} \\ &\quad + ((\omega_1/\omega_3)n_1\gamma_1\cos\theta_1' + (\omega_2/\omega_3)n_2\gamma_2 \\ &\quad \times \cos\theta_2')\mathbf{e}_z^{\Pi}][a_{1x}A_{2x}^{(j)}(z) + a_{2x}^{\Pi}A_{1x}^{(j)}(z) \\ &\quad + a_{1y}A_{2y}^{(j)}(z) + a_{2y}^{\Pi}A_{1y}^{(j)}(z) \\ &\quad + [a_{1z}A_{2z}^{(j)}(z) + a_{2z}A_{1z}^{(j)}(z)]/(n_1n_2)^2] \\ &\quad + [\{f_x^{(j)}(z)\gamma_1 + \alpha_x^{(j)}(z)(\gamma_2-\gamma_1)\}\mathbf{e}_x^{\Pi} \\ &\quad + \{f_y^{(j)}(z)\gamma_2 + \alpha_y^{(j)}(z)(\gamma_2-\gamma_1)\}\mathbf{e}_y^{\Pi} \\ &\quad + \{-\tan\theta_1'\cdot\gamma_1(f_x^{(j)}(z) - \alpha_x^{(j)}(z)) \\ &\quad - \tan\theta_2'\cdot\gamma_2(\alpha_x^{(j)}(z)\cos\alpha_2 - \alpha_y^{(j)}(z)\sin\alpha_2)\}\mathbf{e}_z^{\Pi}] \\ &\quad \times [a_{1x}a_{2x}^{\Pi} + a_{1y}a_{2y}^{\Pi} + a_{1z}a_{2z}/(n_1n_2)^2]/k_3^r\} \end{aligned} \tag{A.14}$$

$$\begin{aligned} \mathbf{P}_{\mathrm{nloc2}}^{(j)}(z) &= [\mathrm{i}\gamma_3/c]\{[(\omega_1/\omega_3)\sin\theta_1 A_{2x}^{(j)}(z) \\ &\quad + a_{2x}^{\Pi}[f_x^{(j)}(z) - \alpha_x^{(j)}(z)]/k_3^r \\ &\quad + a_{2y}^{\Pi}[f_y^{(j)}(z) - \alpha_y^{(j)}(z)]/k_3^r \\ &\quad - \cos\theta_1' A_{2z}^{(j)}(z)(n_1\omega_1)/(n_2^2\omega_3) + a_{2z}\tan\theta_1' \\ &\quad \times [f_x^{(j)}(z) - \alpha_x^{(j)}(z)]/(k_3^r n_2^2)] \\ &\quad \times [a_{1x}\mathbf{e}_x^{\Pi} + a_{1y}\mathbf{e}_y^{\Pi} - (a_{1z}/n_1^2)\mathbf{e}_z^{\Pi}] \\ &\quad + (\omega_1/\omega_3)[a_{2x}^{\Pi}\sin\theta_1 - a_{2z}(n_1/n_2^2)\cos\theta_1'] \\ &\quad \times [A_{1x}^{(j)}(z)\mathbf{e}_x^{\Pi} + A_{1y}^{(j)}(z)\mathbf{e}_y^{\Pi} - (A_{1z}^{(j)}(z)/n_1^2)\mathbf{e}_z^{\Pi}]\} \end{aligned} \tag{A.15}$$

$$\begin{aligned} \mathbf{P}_{\mathrm{nloc3}}^{(j)}(z) &= [\mathrm{i}\gamma_4/c]\{[(\omega_2/\omega_3)\sin\theta_2\cos\alpha_2 A_{1x}^{(j)}(z) \\ &\quad + a_{1x}\alpha_x^{(j)}(z)/k_3^r + (\omega_2/\omega_3)\sin\theta_2\sin\alpha_2 A_{1y}^{(j)}(z) \\ &\quad + a_{1y}\alpha_y^{(j)}(z)/k_3^r - \cos\theta_2' A_{1z}^{(j)}(z) \\ &\quad \times (n_2\omega_2)/(n_1^2\omega_3) + a_{1z}\tan\theta_2' \\ &\quad \times [\alpha_x^{(j)}(z)\cos\alpha_2 + \alpha_y^{(j)}(z)\sin\alpha_2]/(k_3^r n_1^2)] \\ &\quad \times [a_{2x}^{\Pi}\mathbf{e}_x^{\Pi} + a_{2y}^{\Pi}\mathbf{e}_y^{\Pi} - (a_{2z}/n_2^2)\mathbf{e}_z^{\Pi}] \\ &\quad + (\omega_2/\omega_3)[a_{1x}\sin\theta_2\cos\alpha_2 \\ &\quad + a_{1y}\sin\theta_2\sin\alpha_2 - a_{1z}(n_2/n_1^2)\cos\theta_2'] \\ &\quad \times [A_{2x}^{(j)}(z)\mathbf{e}_x^{\Pi} + A_{2y}^{(j)}(z)\mathbf{e}_y^{\Pi} - (A_{2z}^{(j)}(z)/n_2^2)\mathbf{e}_z^{\Pi}]\} \end{aligned} \tag{A.16}$$

$$\begin{aligned} i_x^{(j)}(z) &= -\{b_3[a_{1x}A_{2z}^{(j)}(z) + a_{2z}A_{1x}^{(j)}(z)] \\ &\quad + b_4[a_{1z}A_{2x}^{(j)}(z) + a_{2x}^{\Pi}A_{1z}^{(j)}(z)] \\ &\quad + b_5[a_{1y}A_{2z}^{(j)}(z) + a_{2z}A_{1y}^{(j)}(z)] \\ &\quad - b_6[a_{1z}A_{2y}^{(j)}(z) + a_{2y}^{\Pi}A_{1z}^{(j)}(z)]\} \end{aligned} \tag{A.17}$$

$$\begin{aligned} i_y^{(j)}(z) &= -\{b_3[a_{1y}A_{2z}^{(j)}(z) + a_{2z}A_{1y}^{(j)}(z)] \\ &\quad + b_4[a_{1z}A_{2y}^{(j)}(z) + a_{2y}^{\Pi}A_{1z}^{(j)}(z)] \\ &\quad - b_5[a_{1x}A_{2z}^{(j)}(z) + a_{2z}A_{1x}^{(j)}(z)] \\ &\quad + b_6[a_{1z}A_{2x}^{(j)}(z) + a_{2x}^{\Pi}A_{1z}^{(j)}(z)]\} \end{aligned} \tag{A.18}$$

$$\begin{aligned} i_z^{(j)}(z) &= -\{b_7[a_{2y}^{\Pi}A_{1x}^{(j)}(z) + a_{1x}A_{2y}^{(j)}(z) \\ &\quad - a_{2x}^{\Pi}A_{1y}^{(j)}(z) - a_{1y}A_{2x}^{(j)}(z)] + b_2[a_{2z}A_{1z}^{(j)}(z) \\ &\quad + a_{1z}A_{2z}^{(j)}(z)] + b_1[a_{2x}^{\Pi}A_{1x}^{(j)}(z) \\ &\quad + a_{1x}A_{2x}^{(j)}(z) + a_{2y}^{\Pi}A_{1y}^{(j)}(z) + a_{1y}A_{2y}^{(j)}(z)]\}. \end{aligned} \tag{A.19}$$

New auxiliary coefficients in (A.13)–(A.19) are defined in the following way ($j = x, y; i = x, y$):

$$\begin{aligned} \alpha_x^{(j)}(z) &= f_y^{(j)}(z)w_1^2w_2^2\sin\alpha_2\cos\alpha_2 \\ &\quad \times \tan^2\theta_2/D_0 - f_x^{(j)}(z)w_1^2[w_1^2 + w_2^2(1 + \\ &\quad + \sin^2\alpha_2\tan^2\theta_2)]/(D_0\cos^2\theta_1) \end{aligned} \tag{A.20}$$

$$\begin{aligned} \alpha_y^{(j)}(z) &= f_y^{(j)}(z)\frac{w_1^2(w_2^4\sin^2\alpha_2\cos^2\alpha_2\tan^4\theta_2 - D_0)}{D_0[w_1^2 + w_2^2(1+\sin^2\alpha_2\tan^2\theta_2)]} \\ &\quad - f_x^{(j)}(z)w_1^2[w_1^2 + w_2^2(1 + \\ &\quad + \sin^2\alpha_2\tan^2\theta_2)]/(D_0\cos^2\theta_1) \end{aligned} \tag{A.21}$$

$$A_{1i}^{(j)}(z) = (a_{1xi}[f_x^{(j)}(z) - \alpha_x^{(j)}(z)] + a_{1yi}[f_y^{(j)}(z) - \alpha_y^{(j)}(z)])/k_1^i \quad \text{(A.22)}$$

$$A_{1z}^{(j)}(z) = (a_{1zx}[f_x^{(j)}(z) - \alpha_x^{(j)}(z)] + a_{1zy}[f_y^{(j)}(z) - \alpha_y^{(j)}(z)])/k_1^i \quad \text{(A.23)}$$

$$A_{2i}^{(j)}(z) = (a_{2xi}^{\Pi}\alpha_x^{(j)}(z) + a_{2yi}^{\Pi}\alpha_y^{(j)}(z))/k_2^i \quad \text{(A.24)}$$

$$A_{2z}^{(j)}(z) = (a_{2zx}^{\Pi}\alpha_x^{(j)}(z) + a_{2zy}^{\Pi}\alpha_y^{(j)}(z))/k_2^i. \quad \text{(A.25)}$$

References

[1] Dellwig T, Rupprechter G, Unterhalt H and Freund H-J 2000 *Phys. Rev. Lett.* **85** 776–9
[2] Raschke M B, Hayashi M, Lin S H and Shen Y R 2002 *Chem. Phys. Lett.* **359** 367–72
[3] Roke S, Kleyn A W and Bonn M 2003 *Chem. Phys. Lett.* **370** 227–32
[4] Kuhnke K, Hoffmann D M P, Wu X C, Bittner A M and Kern K 2003 *Appl. Phys. Lett.* **83** 3830–2
[5] Hoffmann D M P, Kuhnke K and Kern K 2002 *Rev. Sci. Instrum.* **73** 3221–6
[6] Flörsheimer M, Brillert C and Fuchs H 1999 *Mater. Sci. Eng.* C **8/9** 335–41
[7] Lozovik Yu E, Merkulova S P, Nazarov M M and Shkurinov A P 2000 *Phys. Lett.* A **276** 127–32
[8] Ostroverkhov V, Waychunas G A and Shen Y R 2005 *Phys. Rev. Lett.* **94** 046102
[9] Wei X, Hong S-C, Zhuang X, Goto T and Shen Y R 2000 *Phys. Rev.* E **62** 5160–72
[10] Lin S H, Hayashi M, Islampour R, Yu J, Yang D Y and Wu G Y C 1996 *Physica* B **22** 191–208
[11] Maki J J, Kauranen M and Persoons A 1995 *Phys. Rev.* B **51** 1425–34
[12] Kauranen M, Verbiest T and Persoons A 1994 *Nonlinear Opt. Princ. Mater. Phenom. Devices* **8** 243
[13] Van Elshocht S, Verbiest T, Kauranen M and Persoons A 1997 *J. Chem. Phys.* **107** 8201–3
[14] Kauranen M, Maki J J, Verbiest T, Van Elshocht S and Persoons A 1997 *Phys. Rev.* B **55** R1985–8
[15] Stolle R, Loddoch M and Marowsky G 1994 *Nonlinear Opt. Princ. Mater. Phenom. Devices* **8** 79
[16] Shen Y R 1999 *Appl. Phys.* B **68** 295
[17] Koroteev N I, Makarov V A and Volkov S N 1997 *Nonlinear Opt. Princ. Mater. Phenom. Devices* **17** 247–69
[18] Golubkov A A and Makarov V A 1996 *J. Russ. Laser Res.* **17** 480–9
[19] Golubkov A A and Makarov V A 1996 *Laser Phys.* **6** 1013–7
[20] Green M, Kirkby P and Timsit R S 1973 *Phys. Lett.* A **45** 259–60
[21] Porras M A 1996 *Opt. Commun.* **131** 13–20
[22] Greffet J J and Baylard C 1992 *Opt. Commun.* **93** 271–6
[23] Kőházi-Kis A 2005 *Opt. Commun.* **253** 28–37
[24] Bliokh K Yu and Bliokh Yu P 2007 *Phys. Rev.* E **75** 066609
[25] Nasalski W 2006 *Phys. Rev.* E **74** 056613
[26] Koroteev N I, Makarov V A and Volkov S N 1997 *Opt. Commun.* **138** 113–7
[27] Koroteev N I, Makarov V A and Volkov S N 1998 *Laser Phys.* **8** 532–5
[28] Makarov V A and Perezhogin I A 2008 *Opt. Commun.* **281** 3906–12
[29] Volkov S N, Makarov V A and Perezhogin I A 2006 *Quantum Electron.* **36** 860–6